



# Superior control for physical properties of sputter deposited ITO thin-films proper for some transparent solar applications

Mohamed Fikry<sup>1,2</sup> · Mohamed Mohie<sup>2</sup> · Menna Gamal<sup>2</sup> · Ahmed Ibrahim<sup>2,3</sup> · Gehad Genidy<sup>4</sup>

Received: 14 October 2020 / Accepted: 28 January 2021 / Published online: 12 February 2021  
© The Author(s), under exclusive licence to Springer Science+Business Media, LLC part of Springer Nature 2021

## Abstract

Superior control of sputtering deposition of ITO thin-films to enhance the physical properties of the ITO thin-films has been investigated. The effect of different sputter deposition conditions and the thermal post-annealing on the physical properties of the transparent-conductive indium tin oxide (ITO) thin-films deposited on a glass substrate have been studied. The power varied from 20 to 210 W with argon (Ar) gas flowing at a rate from 20 to 80 sccm. Thermal post-annealing of deposited thin-films at 200–450 °C in vacuum and air has been carried out as well. The physical properties were monitored using XRD, STM, four-point probe electrometer, and UV–Vis spectrometer. The change of the Ar flow rates influences the deposited films surface roughness, electrical sheet resistance ( $R_s$ ), average optical transmittance ( $T_{avg}$ ) with no apparent change in the morphology fractal dimension. At the Ar flow rate of 30 sccm and the critical power of 120 W, the deposited thin-films transform from amorphous to semi-crystalline structure mostly up 170 W. Optimal thin-films with fairly the highest  $T_{avg}$  at 97.7% and good  $R_s$  with 158.3  $\Omega$ /sq could be obtained under a residual Ar gas flow rate of 50 sccm and at 20 W. The critical post-annealing temperature at 350 °C (air) and 450 °C (vacuum) could initiate the semi-crystalline structure of the previously amorphous deposited thin-films. For the first time, ITO thin-films with  $T_{avg}$  and  $T_{max}$  up to 97.7% and 99.9% respectively have been achieved. Besides, the  $R_s$  value is controlled from 6 to 3981  $\Omega$ /sq with excellent average transparency. These prove viable candidates in transparent solar applications.

**Keywords** ITO thin-film · Magnetron sputtering deposition · RF power · Ar flow rate · Thermal post-annealing · Sheet resistance · Average transmittance

---

✉ Mohamed Fikry  
m\_fikry80@yahoo.com; mfikry@sci.cu.edu.eg

<sup>1</sup> Physics Department, Faculty of Science, Cairo University, Cairo, Egypt

<sup>2</sup> Egypt Nanotechnology Center (EGNC), Cairo University, Cairo, Egypt

<sup>3</sup> NanoScient Technology Company, Nasr City, Cairo, Egypt

<sup>4</sup> Chemistry Department, Faculty of Science, Cairo University, Cairo, Egypt

## 1 Introduction

The technology of materials science can solve many problems in the different parts of life and make the economy in progress. Recently, researchers are interested in the development and discovery of new materials that have eco-friendly properties used in different applications with distinguished specifications (Ettu 2014).

Thin-film technology plays an important role in the nanotechnology, nanoscience development, and particularly in industry. Thin-films are used in several applications such as military coatings, optics, displays, acoustic surveillance, security, aerospace, and semiconductors. Researchers are directed into the thin-film semiconductors technology for their great contribution in many applications of energy like transparent electrodes, photovoltaic devices, solar front panel display, magnetic components, low emissivity coatings for architectural glass, light density memory system for computers, diodes, transistor sensors, various gas sensors, and heat reflectors for advanced gazing in solar cells (Rao and Shekhawat 2013).

Indium tin oxide (ITO) is one of the most relevant thin-films among sustainable eco-friendly semiconductors that have been the subject of many studies lately due to its high transmittance, low electrical resistivity, anti-reflection in visible light (high infrared reflection and UV absorption) (Malik and de la Hidalga-Wade 2017; Siddiqui et al. 2018; Xia and Gerhardt 2016). These properties make ITO thin-films a good candidate for solar applications like coatings in thermal collectors, mirrors, and transparent electrodes. Other technological applications include touch panels electrochromic LCDs, plasma displays, field emission displays, heat reflective coatings, efficient windows, gas sensors, and especially in transparent solar cells (Kaluba et al. 2020; Meiss et al. 2008; Oh et al. 2006; Park et al. 2001; Worasukkhung et al. 2012).

Physical vapor deposition (PVD) and chemical vapor deposition (CVD) techniques are used widely in the production of semiconductors (Dehghanghadikolaei et al. 2018). PVD techniques are preferable processes as they fabricate thin-films with superior hardness, wear resistance, smoothness, withstand high-temperature, and oxidation resistance as well as being eco-friendly. PVD involves several steps performed under a high-temperature vacuum condition. First, a target material is melted typically by high power electricity or laser. Then it is converted into an energetic vapor that falls on the substrate and forms a pure thin coating. The RF magnetron sputtering deposition is the best thin-film fabricated technique because it does not require the use of specialized target materials as used in CVD. Also, its dependence on plasma formation adds benefits to the deposition process (Fikry et al. 2020b; Habig 1986; Malik and de la Hidalga-Wade 2017; Seshan 2001). For instance, DC and RF magnetron sputtering has a wider range of deposition facilities in a pure Ar atmosphere that is simple, cheap and more controllable. Indeed, all inorganic materials such as ITO can be readily deposited which were reported to having good adhesion and low porosity (Films and Box 1982; Malik and de la Hidalga-Wade 2017).

Optical and electrical properties of ITO films vary according to stoichiometry, crystal structure, and film defects under specific deposition conditions of power, substrate temperature, and working residual gas flow rate (Al-Mansoori et al. 2017; Chaoumead et al. 2012; Chityuttakan et al. 2019; Fikry et al. 2020a; Glaswerke 1984; Mientus and Ellmer 2001). Thermal post-annealing effects on the deposited ITO thin-films have been reported as well (Bhagwat and Howson 1999; Kerkache et al. 2006; Meng et al. 1995).

In this paper, we explored the superior control and enhancement of ITO thin-film physical properties by adjusting the RF magnetron sputter deposition parameters such as RF power

and gas flow rate. Meanwhile, thermal post-annealing of deposited films was investigated together with their effect on the structure, electrical and transparent properties. The requirements sought for such ITO film are resistance against scratching, high adhesion to the glass, high stability against environmental influences as well as being fairly cheap. In this context, recommendations have been reported regarding some of the obtained ITO films as viable candidates for ongoing applications based on their properties. These include photovoltaic solar cells, optoelectronic devices, efficient smart windows, geostationary earth orbits satellite, gas sensors, displays, touch screen panels, optics and thermal collectors.

## 2 Methodology

### 2.1 Materials

All samples were deposited on  $7.5 \times 2.5 \text{ cm}^2$  glass slides (Pathmark, 0360–2204), which were cleaned with isopropanol 99% (Organik Kimya) and dried with compressed air. ITO of ratio 90/10 weight % target disk (Protoflex Corporation) of purity 99.99% with 4" diameter and 0.25" thickness has been used as a bulk source of the films.

### 2.2 Sputtering system

ITO films were deposited onto glass substrates by magnetron sputtering (Protoflex Corporation, Flex 1300). The sputtering system has six target source heads of 4" in the sputtering chamber with three RF sources (Advanced Energy, CESAR136) and three DC power supplies (Advanced Energy, MDX 1 K) that can be managed to deposit several film layers with different materials in one process. The sputtering system has RF and DC power ranges up to 600 and 1000 W, respectively. The system allows gas flow rates, deposition temperatures, and sample rotational speeds up to 100 sccm, 800 °C, and 20 rpm, respectively. The distance between the target and substrate was kept constant at 20 cm for each deposition. IR Heater was used for heating the substrate to the required temperature with an incremental rate of 50 °C/min. The chamber and load lock were evacuated by two mechanical rough vacuum pumps (Oerlikon Leybold vacuum), TRIVAC D40 B/ D65 and D16 BCS/ D25 BCS, respectively, to a pressure less than  $2 \times 10^{-2}$  Torr. Besides, a two-compound molecular (turbo) vacuum pump TG220 FRWB and TG1400 FBWB (Osaka vacuum, LTD) were used to maintain the required vacuum pressure of the chamber and load lock, respectively. The turbo vacuum pumps were put in operation after the rough vacuum pumps to reach the base pressure of less than  $2 \times 10^{-6}$  Torr. Evacuation of the sputtering chamber is important for preventing any interaction between plasma sputtering and air molecules, which assure good film deposition. Residual Ar gas flow was adjusted by MKS mass flow (MKS 179A) meter and controller (MKS 1179A and 2179A). When Ar gas flowed into the sputtering chamber, vacuum pressure was decreased to about  $1.5 \times 10^{-3}$  Torr during deposition.

### 2.3 Thin-film investigation

X-ray diffraction (XRD) analysis was carried out by the Bruker D8 discover with Cu-K $\alpha$  graphite monochromatic radiation source ( $\lambda = 1.5418 \text{ \AA}$ ) and operating on  $\theta/2\theta$  configuration of 40 kV and 40 mA with a scan range from 20° to 70° over a step of 0.01°.

A scanning tunneling microscope (STM) (Agilent Technologies, 500LS) with a bias voltage of 0.05 to 0.2 V and set-point current of 1 to 2 nA, was used to explore the topography and morphology of ITO surface films for a high resolution of small-scale scanning.

The electrical sheet resistance of ITO films were measured by a four-probe electrometer (Keithley, 2400) by an average of four readings of I-V curves at different sheet surface positions.

Optical properties (Transmittance and absorbance) of the films were examined by a fiber optic spectrometer (Ocean optics, HR4000 UV-NIR) within ranges of 200 to 1100 nm over approximately 1 nm resolution. A 400  $\mu\text{m}$  diameter optical fiber (Ocean optics, UV-NIR) was used before the dark sample holder to help exclude background radiations. Also, another optical fiber was used to collect the spectrum of films to deliver to the spectrometer.

### 3 Result and discussion

The quality of ITO films depends on many sputtering deposition process conditions such as deposition power, Ar flow rate, and post-annealing (Hammadi 2018; Kosarian et al. 2018). Here the effect of sputtering deposition conditions on the type of structure, morphology, and roughness (RMS) will be discussed together with the extent of their influence on the electrical and transmittance properties of the ITO deposited films. All the deposited ITO films were prepared at a constant deposition time of 30 min and a substrate temperature of 200 °C under vacuum deposition pressure of  $1.5 \times 10^{-3}$  Torr. Meanwhile, RF sputtering power input ranging from 20 to 210 W has been applied while the gas flow rate was set at 30 sccm. Thereupon, an optimal RF deposition power of 20 W was favorably maintained while the gas flow rate was changed gradually from 20 to 80 sccm. Argon gas has been selected as sputtering deposition gas flow because of its mass compatibility with materials of engineering interest and its low cost (Kosarian et al. 2018). Thermal post-annealing of fabricated films has been carried out within a temperature range from 200 to 450 °C under power 20 W and Ar flow rate 50 sccm in vacuum and air.

#### 3.1 XRD crystalline structure investigation

The study of amorphous to crystalline transformation of the ITO films is one of great interest for researchers to understand the microstructural changes and their influence on the physical properties of the films (Xia and Gerhardt 2016). Amorphous materials with complete grain boundaries have excellent mechanical properties (Hammadi 2018; Husain et al. 2018; Malathy et al. 2009; Sathya and Natarajan 2018). Recently, researchers have been focusing on manufacturing amorphous thin-films that reduce the cost by more than half to be used in transparent solar cells due to their higher transmittance (Aviles et al. 2011).

The XRD spectra of ITO thin-films at different conditions revealed two different structures as shown in Fig. 1a–d.

Figure 1a shows that sputtering RF powers up to 80 W resulted in amorphous ITO films with no diffraction peaks except for a barely noticeable peak at 20°. However, the emergence of a diffraction peak at 35° embedded within a hump is reminiscent of the plane (400) due to the  $\text{In}_2\text{O}_3$  cubic crystalline structure (Malathy et al. 2009). It is most likely that 120 W was a critical sputtering RF power at which film structure transforms from amorphous to semi-crystalline. In stark contrast, at 170 W, a poly-crystalline ITO thin-film with a complete transformation of the highly crystalline cubic structure was observed with

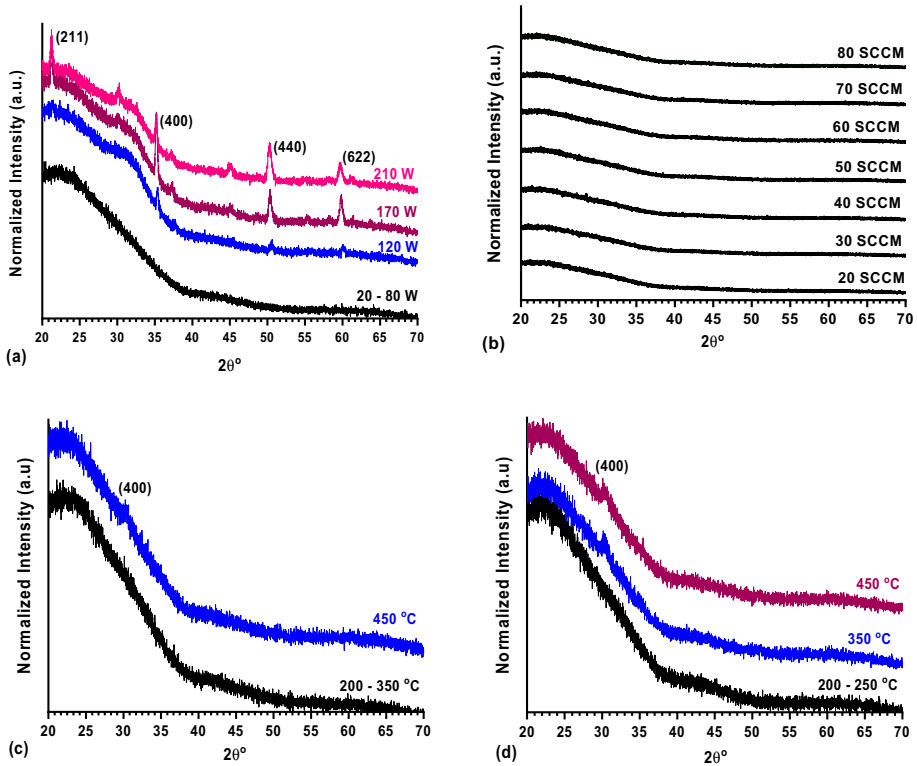


**Fig. 1** XRD spectra of the ITO films at different **a** sputtering RF deposition power, **b** Ar flow rates, thermal annealing in **c** vacuum and **d** air

characteristic peaks corresponding to the planes (211), (400), (440) and (622) according to the reference card (COD 1,538,147). The plane (400) in particular, exhibiting the highest peak intensity (best orientation) proved to have the highest number of atoms and in turn electrons in the unit cell. The increase of the sputtering RF power to 210 W, unfavorably incurs a degradation of the obtained films being less crystalline with lower diffraction peaks intensity. The crystalline size *d* of the ITO crystals can be calculated using the Scherer formula law (Eq. 1) (Pokaipisit et al. 2008),

$$d = K \frac{\lambda}{\beta \cos \theta} \tag{1}$$

where  $\theta$  is the Bragg angle,  $\beta$  is the full width at half max (FWHM in radians) of the peak,  $\lambda$  is the wavelength of the X-ray (0.154 nm) and *K* is the Scherer constant (*K* = 0.9).

Figure 1b displays the effect of Ar flow rate variation on the amorphous structure of ITO thin-films at RF deposition power of 20 W. It turns out that the Ar flow rate variation has no impact on the structure type of ITO thin-films. That it would be attributed to the effect of the Ar flow rate on the deposited ITO thin-film morphology, then the electrical and optical properties due to increase the thickness and the homogeneity of the film with the gas flow rate (Shahidan and Awang 2016).

Thermal post-annealing of ITO thin-films has been carried out at different temperatures in the range from 200 to 450 °C in vacuum and air. In Fig. 1c, d, the appearance of a small hump at 30° can be discerned at annealing temperatures 350 °C and 450 °C in air and vacuum, respectively. This would indicate that a semi-crystalline structure started to grow. The intensity of this hump is relatively higher in air due to ITO thin-film oxidation which promotes atoms to rearrange into a crystalline structure at lower temperatures (Hu et al. 2004).

Table 1 lists XRD parameters of ITO films deposited with RF sputtering powers of 170 and 210 W using origin software. The broadened diffraction peaks with relatively higher  $\beta$  values with smaller crystalline sizes in the case of 210 W sputter power attests to the degradation of film crystallization (Tang et al. 2012; Toma et al. 2019). On the other hand, XRD spectra do not reveal any peaks inherent to Sn, SnO, and SnO<sub>2</sub> traces which indicate tin atoms being doped in the In<sub>2</sub>O<sub>3</sub> lattice (Hammadi 2018). Eventually, it seems that sputtering plasma electron density at RF power about 170 W preferentially produces ITO thin-films with a good crystalline structure.

### 3.2 STM roughness investigation

In the modern research studies, interface roughness (topography) is considered crucial in many physical and chemical properties of thin-films. The high surface roughness and a group of grains can ultimately generate scattering losses for the optical path of the photons or the photoelectrons and also increase the electrons scattering. These would end up reducing their mean free path lengths and thus increasing the sheet resistance of the film (Tang et al. 2012; Toma et al. 2019).

The topography, morphology, and surface roughness of ITO thin-films were studied by STM whereby the fractal dimensions (D) had been calculated by a Box counting technique using Gwyddion software. The STM images of a sputtering deposited ITO thin-films at different physical parameters are displayed in Fig. 2.

In Fig. 2a, thin-films deposited under a sputtering power up to 60 W were characterized by a fine fiber texture structure that developed an initial plane with small accumulation grain sizes which nucleated slowly forming islands at high power sputtering. Moreover, at higher powers from 80 to 170 W, a crystalline structure evolved as grain coarsening occurs during coalescence of small islands with large surface; while grain boundaries disappeared in continuous film growth with layers and islands. However, at the power of 210 W, less island formations can be observed which indicated a lower degree of crystallinity (Zhao et al. 2000).

The effect of the Ar gas flow rate on the morphology of the ITO thin-film surface is shown in Fig. 2b. It is noticed that the surfaces of the films deposited at the Ar flow rate up

**Table 1** The full width at half maximum ( $\beta$ ) and Crystallite size (d) of the crystalline XRD peaks ITO thin-films at sputtering RF deposition powers 170 and 210 W at the XRD peaks

2 $\theta$ °	Structure planes	170 W		210 W	
		$\beta$ (rad)	d (nm)	$\beta$ (rad)	d (nm)
21.275	(211)	0.310	26.023	0.293	27.531
35.215	(400)	0.274	30.310	0.354	23.514
50.332	(440)	0.344	25.443	0.495	17.724
59.821	(622)	0.311	29.420	0.312	29.343

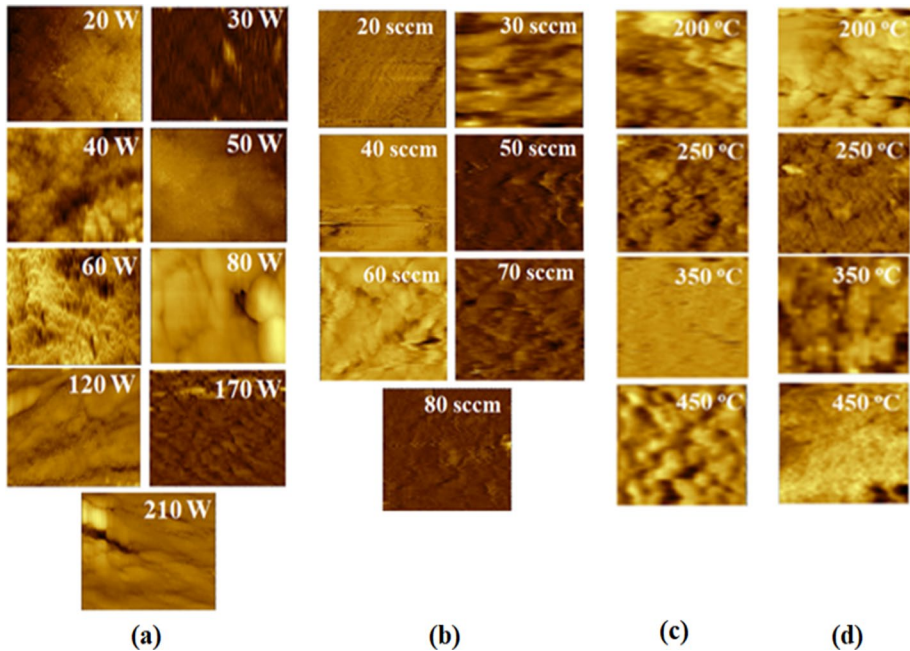


**Fig. 2** STM images of the ITO films at different; **a** sputtering RF deposition power, **b** Ar flow rates, as well as thermal annealing in **c** vacuum and **d** air

to 40 sccm were semi-smooth with a number of remarkable pores at 30 sccm. On the other hand, at higher gas flow rates, the surface diffusion of ITO material on the substrate tends to increase which results in atoms forming bonds with each other so that the film becomes less rough (Al-Mansoori et al. 2017).

Figure 2c, d displays the effect of thermal post-annealing on ITO thin-film morphology in vacuum (Fig. 2c and air Fig. 2d) at different temperatures ranging from 200 to 450 °C. In vacuum, the diffusion of ITO particles on the surface of the substrate tends to form bonds between particles which increases with raising the annealing temperature from 200 to 350 °C. Then, nucleation seems to start at 450 °C. In contrast, thermal post-annealing in air favors the enhancement of ITO thin-film adhesions at 200 °C and 250 °C. As annealing temperature was increased to 350 °C, the nucleation of ITO particles forms grains whereby converting ITO thin-film from amorphous to semi-crystalline structure. This structural transformation tends to continue as temperature increases up to 450 °C. All of these STM findings corroborate previous XRD spectra results.

Fractal dimension ( $D$ ) is a measure of complexity that indicates the degree of which the objects fill the available space (surface profile). It is also a parameter to describe the thin-film surface density by the number of grains along the area of growing thin-film. An object with  $D=1$  is meant to be a one-dimensional object. The dimension  $D=2$  describes plane objects while dimension  $D=3$  defines three-dimensional objects as a bulk material. A smaller value of  $D$  means a smoother surface. The fractal dimension characterizes the degree of the surface roughness and can be calculated from the Eq. (2) (Raoufi 2009);

$$D = \frac{\log N}{\log h} \tag{2}$$

where  $N$  is the number of forming shapes for counting and  $h$  is the studied area. It is the slope of  $\log N$  versus  $\log h$  relation as depicted in Fig. 3a–d. Table 2 summarizes the calculated fractal dimensions of ITO thin-films.

From Table 2, the nearly equal  $D$  values obtained under different experimental conditions still indicate that the ITO samples behave as planar objects.

The variation of roughness root mean square (RMS) of ITO films under different deposition conditions is shown in Fig. 4.

Figure 4a, b, d demonstrate that roughness RMS values decrease by increasing both RF power, Ar flow rate, and post annealing temperature in air. This is associated with uniform distribution of grain growth due to crystallinity (Khanal 2016)(Eshaghi et al. 2010) and bonding (Al-Mansoori et al. 2017) with smoother surface formation as sputtering power and Ar gas flow increase. The roughness RMS of ITO thin-films tends to behave differently with post annealing temperature in vacuum as shown in Fig. 4c. In vacuum, for instance, a hump like relation appears where RMS roughness culminates (~0.175 nm) at an annealing temperature of 350 °C. There seems to spreading, accumulation of particles before

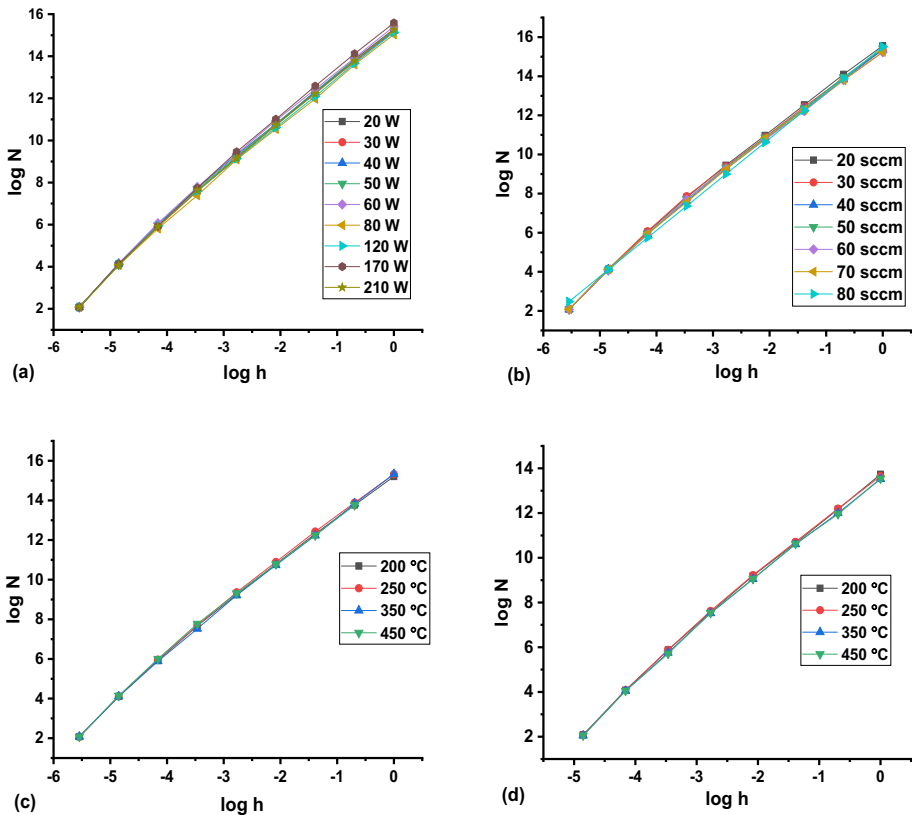
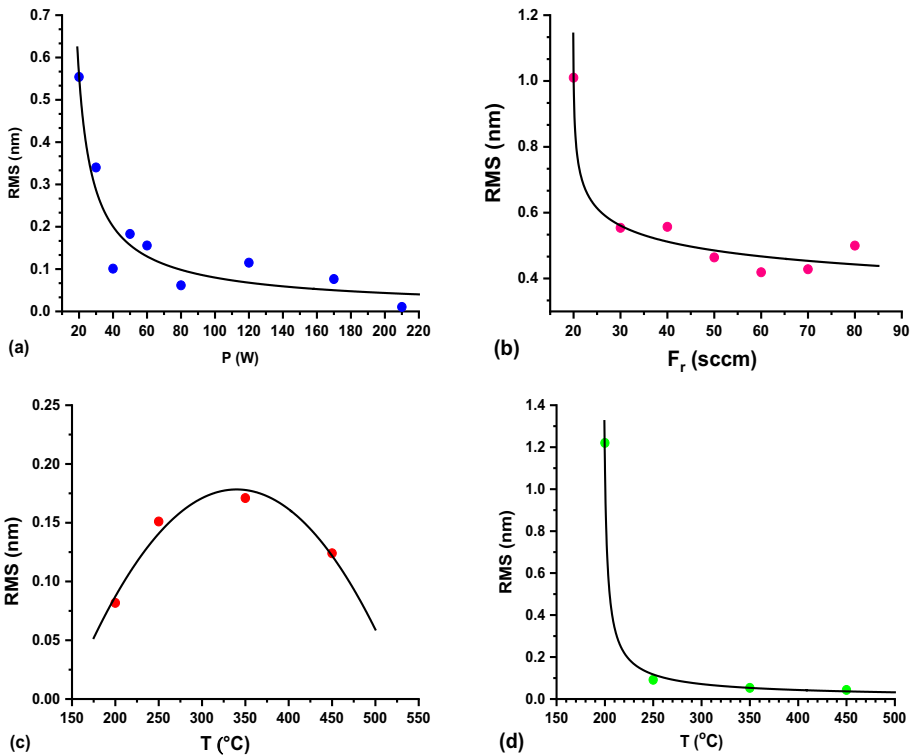


Fig. 3 Relation between  $\log N$  and  $\log h$  at different; **a** sputtering RF deposition power, **b** Ar flow rates, as well as thermal annealing from in **c** vacuum and **d** air



**Table 2** The fractal dimension (D) of the manufactured ITO thin-films variations at different sputtering RF power (P), Ar flow rates ( $F_r$ ) and Thermal annealing (T) in vacuum (VA) and air (AA)

P (W)	20	30	40	50	60	80	120	170	210
D	2.352	2.334	2.332	2.395	2.369	2.346	2.312	2.318	2.305
$F_r$ (sccm)	20	30	40	50	60	70	80		
D	2.404	2.362	2.361	2.378	2.342	2.347	2.349		
T (°C)			200	250	350	450			
D	VA	2.341	2.366	2.358	2.372				
	AA	2.370	2.365	2.338	2.356				



**Fig. 4** Variation of RMS roughness of the ITO thin-films at different; **a** sputtering RF deposition power, **b** Ar flow rates, as well as thermal annealing in **c** vacuum and **d** air

the nucleation and eventual transformation from amorphous to semi-crystalline structure. Besides, at higher temperatures, an increase in the degree of crystallization (Khanal 2016; Mohamed et al. 2009) would occur. However, ITO films thermally annealed in air tend to be rougher than in vacuum at low post-annealing temperatures due to the formation of amorphous oxide film (Hu et al. 2004)(Aviles et al. 2011; Peter and Maan 2016).

### 3.3 Optical and electrical properties investigation

Charge carriers of ITO thin-films are the main parameter that affects transmittance and sheet resistance (Eshaghi et al. 2010). The sheet resistance  $R_s$  can be evaluated from Eq. (3);

$$R_s = R C_f \quad (3)$$

where  $R$  is the average measured resistance by Keithley at some points all-over the thin-film and  $C_f \sim 0.95205$  is a correction factor (Ossila Ltd 2021).

A figure of merit ( $FOM_{(H-HR)}$ ) has been adopted to evaluate the performance or effectiveness of transparent conductive ITO films (TCFs) with different optical and electrical properties as follows;

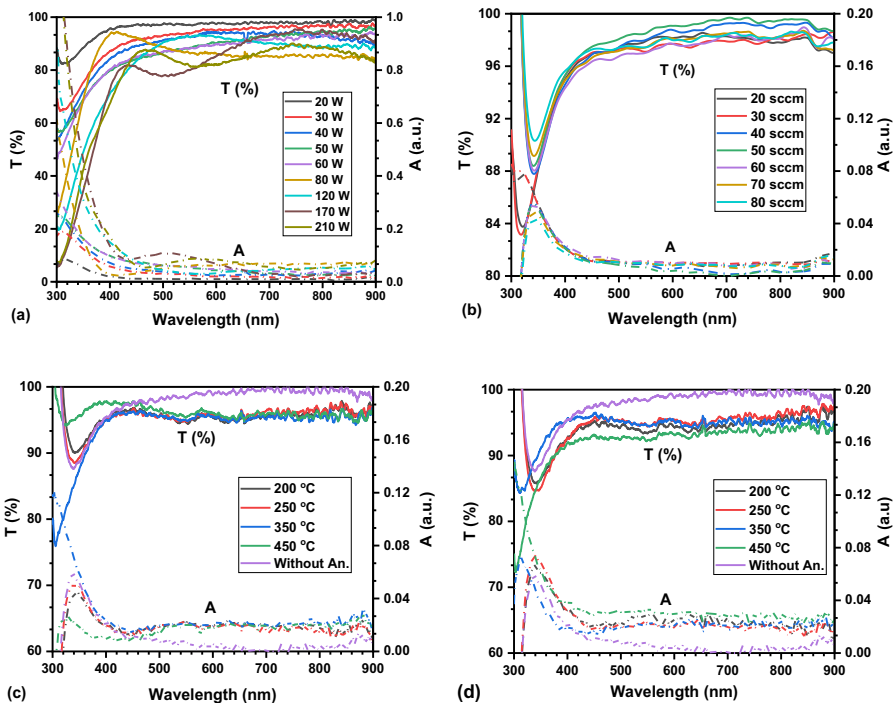


**Fig. 5** Optical transmittance (solid lines) and absorbance (dash lines) spectra of ITO films at different; **a** sputtering RF deposition power, **b** Ar flow rates, as well as thermal annealing in **c** vacuum and **d** air

$$FOM_{(H - HR)} = \frac{T_{avg}}{\sqrt[n]{R_s}} \tag{4}$$

where  $n=10$  (Cisneros-Contreras et al. 2019) while  $T_{avg}$  and  $R_s$  denote the film average transmittance and sheet resistance respectively.

Figure 5a–d displays the behavior of optical VIS–NIR transmittance and absorbance of ITO thin-films at different experimental conditions of sputtering RF deposition power, Ar flow rates as well as after post-annealing at different temperatures in a vacuum and air. The transmittance of all deposited films was found to be higher than 80% and as high as 97.2% at the standard wavelength of 550 nm. Absorbance accounts for about half of the remaining percentage of light intensity so that the reflection was to be equal to absorption. The effects of the sputtering deposition parameters and the thermal post-annealing in vacuum and air on the average transmittance and sheet resistance are illustrated in Fig. 6.

Figures 5a and 6a, show that thin-films average transmittance decrease with RF power at a faster pace by about 11% at 80 W followed by a slower decrement of 2.5% at 210 W with less resistance due to higher degree of crystallinity of the deposited ITO thin-films (Peter and Maan 2016; Raoufi 2009). Furthermore, the transformation of the ITO films from the amorphous to crystalline structure improved the probability of Sn<sup>4+</sup> doping with In<sup>3+</sup> ions in In<sub>2</sub>O<sub>3</sub> sites (Lee and Ok Park 2006). Spectral transmittance in the range of (400–900 nm) tends to be more susceptible to variations by about 23% at the lowest deposition RF power of 20 W. Likewise, thin-films sheet resistance  $R_s$  abruptly decreased with

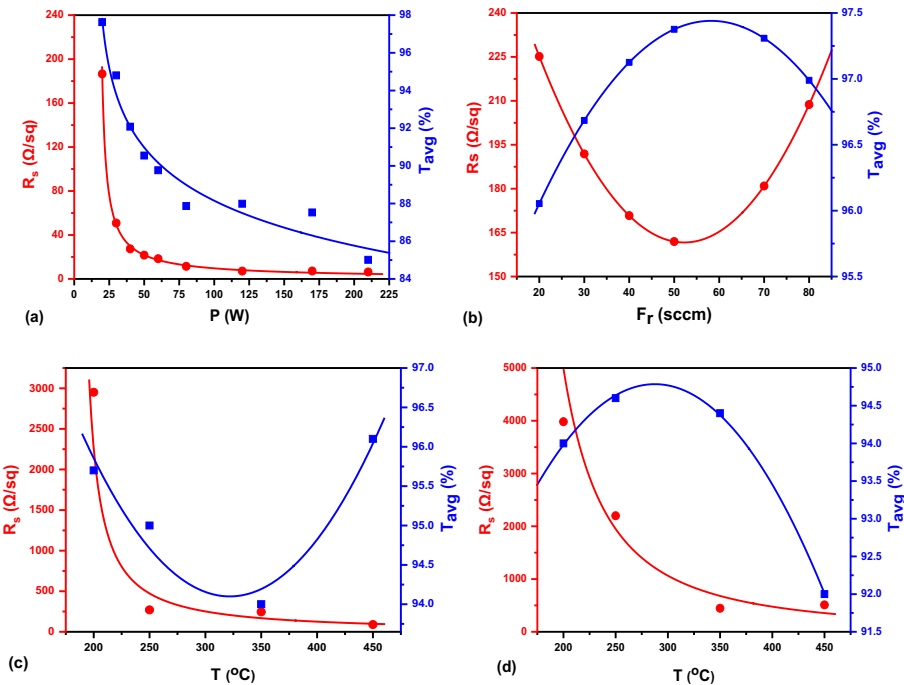


**Fig. 6** Variation of sheet resistance  $R_s$  (red lines) and average transmittance  $T_{avg}$  (blue lines) of the ITO thin-films at different; **a** sputtering RF deposition power, **b** Ar flow rates, as well as thermal annealing in **c** vacuum and **d** air

increasing RF deposition power as earlier as 40 W down to 27.3  $\Omega/\text{sq}$  and then to 6.3  $\Omega/\text{sq}$  at 210 W. Higher sheet resistance of ITO thin-films deposited at lower sputter power because of trapped the electrons in the net of short-range non-crystalline as well as non-uniform films structure and the higher surface roughness RMS. At higher sputter powers, ITO films with a poly-crystalline structure (improvement for film density) of larger thickness would lead to higher mobility of electrons to take place and lower sheet resistance (Bingel et al. 2013).

As clearly shown in Fig. 6b favorable ITO films with the highest transmittance and a small sheet resistance can be preferentially obtained under the condition of deposition with Ar gas flowing at a rate of 50 sccm. At this level of gas flow rate, ITO thin-films exhibit about 97.3% of average transmittance and 158.3  $\Omega/\text{sq}$  sheet resistance. Critical surface roughness and thickness variation as well as carrier concentration (Ar gas) are likely to induce this type of changeover in behavior (Tien et al. 2018; Bhardwaj et al. 2018; Farhan et al. 2013).

A similar trend could be observed due to variations in ITO films post-annealing temperatures in vacuum or air as shown in Fig. 6c, d. The sheet resistance tends to decrease with increasing post-annealing temperature from 2951.9 to 88.8  $\Omega/\text{sq}$  in vacuum and from 3981.6 to 511.8  $\Omega/\text{sq}$  in air. This considerable decline is associated with ITO films transition from amorphous to semi-crystalline structure. Yet, relatively high value of  $R_s$  of the ITO films post-annealed in air is due to amorphous oxide semiconductors less roughness RMS and formed of tail states in the band gap. For the average transmittance, a counter-acting effects of post-annealing in vacuum and air occur around a temperature of 350 °C. Lower values at higher post-annealing temperatures are reflections of the lower and higher degree of roughness and crystallinity of ITO films respectively (Khanal 2016; Eshaghi et al. 2010; Mohamed et al. 2009).

In the light of previous experimental findings, fabricated ITO films reveal versatile characteristics viable to potential applications. These can be classified in terms of experimental conditions of sputtering power level  $P(x)$ , residual gas flow rate  $F(x)$  and post-annealing temperature in air AA(T) or vacuum AV(T). Thereupon, some ITO thin-films are characterized by a very high max transmittance up to 99.9% such as  $P(20)F_r(50)$ ,  $P(20)F_r(70)$  and  $P(20)F_r(50)AA(250)$ . On the other hand, samples with  $P(210)F_r(30)$  have the smallest sheet resistance within value of 6.2  $\Omega/\text{sq}$ .

ITO thin-film sample deposited at  $P(20)F_r(50)$  show higher average transparency, acceptable sheet resistance, and RMS roughness up to 97.7%, 158.3  $\Omega/\text{sq}$ , and 0.46 nm respectively. These are good candidates in many optical applications (Cisneros-Contreras et al. 2019; Meiss et al. 2008).

Besides, films with  $T_{\text{avg}} > 80\%$ ,  $R_s < 310 \Omega/\text{sq}$  and  $FOM_{(H-HR)} > 0.45 (\Omega/\text{sq})^{1/10}$  are acceptable for flat panel displays (FPDs), liquid crystal displays (LCDs), touch screen panels, transparent photovoltaic solar cells, light-emitting diodes (LEDs), gas sensors, efficient smart windows, thermal collectors and thermal mirrors applications (Ali et al. 2014; Cisneros-Contreras et al. 2019).

ITO films with higher  $FOM_{(H-HR)}$  prove favorably feasible in previously mentioned potential applications as well. In this regard,  $FOM_{(H-HR)} \sim 0.73057 (\Omega/\text{sq})^{1/10}$  at  $P(120)F_r(30)$  is considered as the best fabricated ITO film sample suited for optoelectronic devices. Though the ITO thin-film deposited at a gas flow rate of 50 sccm was preferable, fabricated ITO thin-films under different Ar flow rates are nonetheless acceptable for many optoelectronic devices and solar cell applications.  $FOM_{(H-HR)}$  of ITO Thin-films slightly changes with Ar flow rate variations. However, as deposited ITO films annealing at 450 °C in vacuum was tended to increase  $FOM_{(H-HR)}$  up to 0.613 which indicated an improvement

of their efficiency. Moreover, Semi-crystalline ITO Thin-films annealed at 450 °C in vacuum seem to have the highest transparency with good electrical sheet resistance and RMS roughness. It is worth noting that ITO films having  $R_s$  within the range of 2 to 10 k $\Omega$ /sq are considered efficient optical solar reflector (OSR) for space applications, especially in geostationary earth orbits (GEO) satellite applications (Sibin et al. 2016).

## 4 Conclusion

Different ITO thin-films were sputter deposited on a glass substrate at a constant substrate temperature of 200 °C and a residual Ar gas at  $\sim 2 \times 10^{-3}$  Torr vacuum. The processing conditions of a magnetron sputtering deposition such as RF power and Ar flow rate had directly affected the structure, surface morphology, transmittance and sheet resistance of deposited films. The increase of the RF sputtering powers led to increase the electrical conductivity and slightly decrease the transparency with transform the amorphous structure to crystalline. The thin-films assume a semi-crystalline structure at a critical power of about 120 W and their best crystalline structure at 170 W. On the other hand, increasing sputtering power up to 210 W tends to have negative effects on the crystallinity of films. Ar flow rate variation led to a different manner of variations in the films transmittance and sheet resistance. Optimal deposited ITO thin-film transmittance with average 97.7% and max 99.9% as well as 158.3  $\Omega$ /sq sheet resistance could be obtained at 20 W and 50 sccm. On the other hand, the lowest sheet resistance  $\sim 6$   $\Omega$ /sq was achieved at 210 W RF power and 30 sccm Ar flow rate with 85% average transmittance. The crystallization critical post-annealing temperature in air amounts to 350 °C which was lower than under vacuum at 450 °C. The highly optimized ITO thin-film for optoelectronic devices could be produced at 120 W RF power under a residual Ar gas flow rate of about 30 sccm having 89% average transmittance, 7.11  $\Omega$ /sq sheet resistance and  $FOM_{(H-HR)} = 0.73$  ( $\Omega$ /sq)<sup>1/10</sup>. Besides, deposited films were annealed at 200 °C (Vacuum) and 200, 250 °C (air) results in an excellent sheet resistance about 2–4 k $\Omega$ /sq with average solar transmittance 94–96% which are favorably suited for space applications. ITO thin-film samples P(20)F<sub>r</sub>(50), P(20)F<sub>r</sub>(70), and P(20)F<sub>r</sub>(50)AA(250) are characteristic by a very high max transmittance up to 99.9%.

## References

- Al-Mansoori, M., Al-Shaibani, S., Al-Jaedi, A., Lee, J., Choi, D., Hasoon, F.S.: Effects of gas flow rate on the structure and elemental composition of tin oxide thin films deposited by RF sputtering. *AIP Adv.* **7**, 125105 (2017). <https://doi.org/10.1063/1.5001883>
- Ali, A.H., Shuhaimi, A., Hassan, Z.: Structural, optical and electrical characterization of ITO, ITO/Ag and ITO/Ni transparent conductive electrodes. *Appl. Surf. Sci.* **288**, 599–603 (2014). <https://doi.org/10.1016/j.apsusc.2013.10.079>
- Aviles, T., Lethien, C., Zegaoui, M., Vilcot, J.P., Leroy, F., Roussel, P., Rolland, N., Rolland, P.A.: Recent developments in amorphous sputtered ITO thin films acting as transparent front contact layer of CIGS solar cells for energy autonomous wireless microsystems. In: *Conf. Rec. IEEE Photovolt. Spec. Conf.*, pp. 1235–1237 (2011). <https://doi.org/10.1109/PVSC.2011.6186180>
- Bhagwat, S., Howson, R.P.: Use of magnetron-sputtering technique for the control of the properties of indium tin oxide thin films. *Surf. Coat. Technol.* **111**, 163–171 (1999). [https://doi.org/10.1016/S0257-8972\(98\)00727-0](https://doi.org/10.1016/S0257-8972(98)00727-0)

- Bhardwaj, S., Basumatary, P., Agarwal, P.: Influence of argon flow rate on structural and optical properties of TiO<sub>2</sub> thin films deposited by RF sputtering. *AIP Conf. Proc.* **1953**, 1–5 (2018). <https://doi.org/10.1063/1.5032979>
- Bingel, A., Fücksel, K., Kaiser, N., Tünnermann, A.: Pulsed DC magnetron sputtering of transparent conductive oxide layers. *Chin. Opt. Lett. COL* **11**, S10201 (2013). <https://doi.org/10.3788/COL201311.S10201>
- Chaoumead, A., Sung, Y.M., Kwak, D.J.: The effects of RF sputtering power and gas pressure on structural and electrical properties of ITO thin film. *Adv. Condens. Matter Phys.* **2012**, 651587 (2012). <https://doi.org/10.1155/2012/651587>
- Chityuttakan, C., Chinvetkitvanich, P., Chatraphorn, S., Chatraphorn, S.: Influence of deposition parameters on the quality of ITO films for photovoltaic application. *AIP Conf. Proc.* **2091**, 020016 (2019)
- Cisneros-Contreras, I.R., Muñoz-Rosas, A.L., Rodríguez-Gómez, A.: Resolution improvement in Haacke's figure of merit for transparent conductive films. *Results Phys.* **15**, 102695 (2019). <https://doi.org/10.1016/j.rinp.2019.102695>
- Dehghanghadikolaei, A., Ansary, J., Ghoreishi, R.: Sol-gel process applications: a mini-review. *Proc. Nat. Res. Soc.* **2**, 1–11 (2018). <https://doi.org/10.11605/j.pnrs.201802008>
- Eshaghi, A., Pakshir, M., Mozaffarinia, R.: Preparation and photo-induced super hydrophilicity of composite TiO<sub>2</sub>-SiO<sub>2</sub>-In<sub>2</sub>O<sub>3</sub> thin film. *Appl. Surf. Sci.* **256**, 7062–7066 (2010). <https://doi.org/10.1016/j.apsusc.2010.05.026>
- Ettu, E.O.: The role/importance of engineering materials utilization in present day world. *Int. J. Eng. Dev. Res.* **3**, 308–323 (2014)
- Farhan, M.S., Zalnezhad, E., Bushroa, A.R., Aly, A., Sarhan, D.: Electrical and optical properties of indium-tin oxide (ITO) Films by ion-assisted deposition (IAD) at room temperature. *Int. J. Precis. Eng. Manuf.* **14**, 1465–1469 (2013). <https://doi.org/10.1007/s12541-013-0197-5>
- Fikry, M., Tawfik, W., Omar, M.: Measurement of the electron temperature in a metallic copper using ultrafast laser-induced breakdown spectroscopy. *J. Russ. Laser Res.* **41**, 484–490 (2020a). <https://doi.org/10.1007/s10946-020-09901-w>
- Fikry, M., Tawfik, W., Omar, M.M.: Investigation on the effects of laser parameters on the plasma profile of copper using picosecond laser induced plasma spectroscopy. *Opt. Quantum Electron.* **52**, 249 (2020b). <https://doi.org/10.1007/s11082-020-02381-x>
- Films, T.S., Box, O.:  $T \sim J^\circ$ . **90**, 317–321 (1982)
- Glaswerke, S.: Schott Glaswerke, Hattenbergstr. 10, 6500 Mainz, FRG. **63**, 243–249 (1984)
- Habig, K. -H.: Chemical vapor deposition and physical vapor deposition coatings: properties, tribological behavior, and applications. *J. Vac. Sci. Technol. A Vacuum, Surf., Film.* **4**, 2832–2843 (1986). <https://doi.org/10.1116/1.573687>
- Hammadi, O.: Fundamentals of Plasma Sputtering. (2018). <https://doi.org/10.13140/RG.2.1.3855.5605>
- Hu, Y., Diao, X., Wang, C., Hao, W., Wang, T.: Effects of heat treatment on properties of ITO films prepared by rf magnetron sputtering. *Vacuum* **75**, 183–188 (2004). <https://doi.org/10.1016/j.vacuum.2004.01.081>
- Husain, A.A.F., Hasan, W.Z.W., Shafie, S., Hamidon, M.N., Pandey, S.S.: A review of transparent solar photovoltaic technologies. *Renew. Sustain. Energy Rev.* **94**, 779–791 (2018). <https://doi.org/10.1016/j.rser.2018.06.031>
- Kaluba, V.S., Mohamad, K., Ferrer, P.: Experimental and simulated performance of hot mirror coatings in a parabolic trough receiver. *Appl. Energy.* **257**, 114020 (2020). <https://doi.org/10.1016/j.apenergy.2019.114020>
- Kerkache, L., Layadi, A., Dogheche, E., Rémiens, D.: Physical properties of RF sputtered ITO thin films and annealing effect. *J. Phys. D: Appl. Phys.* **39**, 184–189 (2006). <https://doi.org/10.1088/0022-3727/39/1/027>
- Khanal, R.: Properties of amorphous transparent conducting and semiconducting oxides from first principles, vol. 2539, pp. 1–180 (2016)
- Kosarian, A., Shakiba, M., Farshidi, E.: Role of sputtering power on the microstructural and electro-optical properties of ITO thin films deposited using DC sputtering technique. *IEEJ Trans. Electr. Electron. Eng.* **13**, 27–31 (2018). <https://doi.org/10.1002/tee.22494>
- Lee, H.C., Ok Park, O.: The evolution of the structural, electrical and optical properties in indium-tin-oxide thin film on glass substrate by DC reactive magnetron sputtering. *Vacuum* **80**, 880–887 (2006). <https://doi.org/10.1016/j.vacuum.2005.11.069>
- Malathy, V., Sivaranjani, S., Vidhya, V.S., Prince, J.J., Balasubramanian, T., Sanjeeviraja, C., Jayachandran, M.: Amorphous to crystalline transition and optoelectronic properties of nanocrystalline indium tin oxide (ITO) films sputtered with high rf power at room temperature. *J. Non. Cryst. Solids.* **355**, 1508–1516 (2009). <https://doi.org/10.1016/j.jnoncrysol.2009.04.043>

- Malik, O., de la Hidalga-Wade, F.J.: Sputtered indium tin oxide films for optoelectronic applications. In: Optoelectron. Adv. Device Struct. vol. 297 (2017)
- Meiss, J., Urrich, C.L., Fehse, K., Pfuetzner, S., Riede, M.K., Leo, K.: Transparent electrode materials for solar cells. *Photon. Sol. Energy Syst. II.* **7002**, 700210 (2008). <https://doi.org/10.1117/12.781275>
- Meng, L., Macarico, A., Martins, R.: Study of annealed indium tin oxide films prepared by RF reactive magnetron sputtering. *Mater. Res. Soc. Symp.* - Proc. **388**, 379–384 (1995)
- Mientus, R., Ellmer, K.: Reactive magnetron sputtering of tin-doped indium oxide (ITO): Influence of argon pressure and plasma excitation mode. *Surf. Coat. Technol.* **142–144**, 748–754 (2001). [https://doi.org/10.1016/S0257-8972\(01\)01160-4](https://doi.org/10.1016/S0257-8972(01)01160-4)
- Mohamed, S.H., El-Hossary, F.M., Gamal, G.A., Kahlid, M.M.: Properties of indium tin oxide thin films deposited on polymer substrates. *Acta Phys. Pol. A.* **115**, 704–708 (2009). <https://doi.org/10.12693/APhysPolA.115.704>
- Oh, B.Y., Jeong, M.C., Moon, T.H., Lee, W., Myoung, J.M., Hwang, J.Y., Seo, D.S.: Transparent conductive Al-doped ZnO films for liquid crystal displays. *J. Appl. Phys.* **99**, 124505 (2006) <https://doi.org/10.1063/1.2206417>
- Ossila Ltd: Sheet Resistance Equations and Theory: Complete Guide. <https://www.ossila.com/pages/sheet-resistance-theory#measuring-sheet-resistance> (2021)
- Park, S.K., Han, J.I., Kim, W.K., Kwak, M.G.: Deposition of indium-tin-oxide films on polymer substrates for application in plastic-based flat panel displays. *Thin Solid Films* **397**, 49–55 (2001). [https://doi.org/10.1016/S0040-6090\(01\)01489-4](https://doi.org/10.1016/S0040-6090(01)01489-4)
- Peter, A., Maan, A.: Effects of film thickness and sputtering power on properties of ITO thin films deposited by RF magnetron sputtering without oxygen. *J. Mater. Sci. Mater. Electron.* **27**, 11064–11071 (2016). <https://doi.org/10.1007/s10854-016-5223-9>
- Pokaipisit, A., Horprathum, M., Limsuwan, P.: Vacuum and air annealing effects on properties of indium tin oxide films prepared by ion-assisted electron beam evaporation. *Jpn. J. Appl. Phys.* **47**, 4692–4695 (2008). <https://doi.org/10.1143/JJAP.47.4692>
- Rao, M.C., Shekhawat, M.S.: a Brief Survey on Basic Properties of Thin Films for Device Application. *Int. J. Mod. Phys. Conf. Ser.* **22**, 576–582 (2013). <https://doi.org/10.1142/s2010194513010696>
- Raoufi, D.: Morphological characterization of ITO thin films surfaces. *Appl. Surf. Sci.* **255**, 3682–3686 (2009). <https://doi.org/10.1016/j.apsusc.2008.10.020>
- Sathya, P., Natarajan, R.: Design and optimization of amorphous based on highly efficient HIT Solar Cell. *Appl. Sol. Energy (English Transl. Geliotekhnika)*. **54**, 77–84 (2018). <https://doi.org/10.3103/S0003701X18020123>
- Seshan, K.: Handbook of thin film deposition processes and techniques. William Andrew (2001)
- Shahidan, M.F.S., Awang, R.: Effect of Argon-oxygen flow rate ratio in magnetron sputtering on morphology and hygroscopic property of SnO<sub>2</sub> thin film. *Int. J. Electrochem. Sci.* **11**, 6886–6901 (2016). <https://doi.org/10.20964/2016.08.45>
- Sibin, K.P., Swain, N., Chowdhury, P., Dey, A., Sridhara, N., Shashikala, H.D., Sharma, A.K., Barshilia, H.C.: Optical and electrical properties of ITO thin films sputtered on flexible FEP substrate as passive thermal control system for space applications. *Sol. Energy Mater. Sol. Cells.* **145**, 314–322 (2016). <https://doi.org/10.1016/j.solmat.2015.10.035>
- Siddiqui, M.S., Saxena, A.K., Singh, S.P.: Deposition and characterization of ITO thin film over glass for fogger application and for solar photovoltaics. *Int. J. Curr. Eng. Technol.* **8**, 4–8 (2018). <https://doi.org/10.14741/ijcet/v.8.4.1>
- Tang, W., Chao, Y., Weng, X., Deng, L., Xu, K.: Optical property and the relationship between resistivity and surface roughness of indium tin oxide thin films. *Phys. Procedia.* **32**, 680–686 (2012). <https://doi.org/10.1016/j.phpro.2012.03.618>
- Tien, C.L., Lin, H.Y., Chang, C.K., Tang, C.J.: Effect of oxygen flow rate on the optical, electrical, and mechanical properties of DC sputtering ITO thin films. *Adv. Condens. Matter Phys.* **2018**, 2647282 (2018). <https://doi.org/10.1155/2018/2647282>
- Toma, M., Ursulean, N., Marconi, D., Pop, A.: Structural and optical characterization of Cu doped ZnO thin films deposited by RF magnetron sputtering. *J. Electr. Eng.* **70**, 127–131 (2019). <https://doi.org/10.2478/jee-2019-0054>
- Worasukkhung, S., Pudwat, S., Eiamchai, P., Horprathum, M., Dumrongrattana, S., Aiempnanakit, K.: Hydrophilic property of TiO<sub>2</sub> films sputtered on glass/ITO for self-cleaning glass and heat mirror application. *Procedia Eng.* **32**, 780–786 (2012). <https://doi.org/10.1016/j.proeng.2012.02.012>
- Xia, N., Gerhardt, R.A.: Fabrication and characterization of highly transparent and conductive indium tin oxide films made with different solution-based methods. *Mater. Res. Express.* **3**, 1–11 (2016). <https://doi.org/10.1088/2053-1591/3/1/116408>

Zhao, Y., Wang, G.-C., Lu, T.-M.: Characterization of Amorphous and Crystalline Rough Surface-Principles and Applications, vol. 37. Elsevier, Amsterdam (2000)

**Publisher's Note** Springer Nature remains neutral with regard to jurisdictional claims in published maps and institutional affiliations.